J MATER SCI **41** (2006) 1363–1368

Direct fabrication of anatase/activated carbon nano-hybrid materials by hydrothermal with ball milling method at low temperature

N. SAKAMOTO, T. FUJINO, T. WATANABE, M. YOSHIMURA
Materials and Structures Laboratory, Tokyo Institute of Technology, 4259 Natastuta, Midori-ku, Yokohama, 228-8503, Japan
E-mail: n-saka@msl.titech.ac.jp
E-mail: yoshimura@msl.titech.ac.jp

Nano-hybrid materials of anatase and activated carbon were fabricated in a single step by a hydrothermal with ball milling method (H with B) using a conventional autoclave and SiC balls at 180°C. To investigate the influence of ball milling and activated carbon, a hydrothermal method without ball milling (H without B) and a carbonless hydrothermal method with ball milling (Carbonless H with B) were performed. By comparing the three samples based on Transmission Electron Microscopy (TEM) observation and Selected Area Electron Diffraction (SAED) analysis, it was revealed that TiO_2 particles in the hybrid materials heterogeneously nucleate on the activated carbon and have a tendency of crystal growth along the *c* axis under the given experimental condition. The crystal growth direction was controlled isotropically by assisting the ball milling during reaction. The balls seem to act as a stirrer rather than a grinder for the sample containing the activated carbon.

1. Introduction

TiO_2 nano-particles are currently very interesting particularly in the area of photocatalysis. For this application, the size and morphology of the TiO_2 particles are very important [1]. The combination of TiO_2 with some supports has been considered to be effective for this purpose. The synergetic effects of the hybrid materials of TiO_2 particles and adsorbents, such as activated carbon, silica gel, zeolite, etc., have attracted the attention of scientists and engineers because of their higher photocatalytic activity during the decomposition of various environmental pollutants in gas and liquid phases than only TiO_2 particles [2, 3]. Recently, many researchers have reported the fabrication of hybrid materials by chemical vapor deposition [3], the ionized cluster beam method [4] or wet mixing under hydrothermal conditions [5]. However, gaseous processings particularly using vacuum systems require huge amounts of energy to fabricate these hybrid materials. Generally speaking, solution techniques consume less energy than gaseous ones [6–8], however, previous research has used multiple steps; first precipitating TiO_2 particles and then mixing them with activated carbon to fabricate the TiO_2/carbon hybrids. These multistep fabrications waste more energy than single step ones because every step has its own equipment and procedures. Prezepiorski *et al.* reported the fabrication of these hybrids by a single step method, in which the activation of coal and precipitation of TiO_2 powders from a titanium sol were achieved in a gaseous stream [9]. Thus, this method still requires the complex preparations of the precursor and a special setup for the strict control of the nitrogen gas and steam flow.

Our group has studied the fabrication of these hybrids or composites in a single step under hydrothermal conditions. We have succeeded in fabricating TiO_2/ hydroxyapatite composites in a single step [10]. In the present study, we achieved the direct fabrication of TiO_2/activated carbon materials by a conventional hydrothermal method and a hydrothermal with ball milling method. In this hydrothermal process with ball milling, the sample can be vigorously stirred during fabrication using rotating balls in a conventional autoclave. We now report the effects of

0022-2461
DOI: 10.1007/s10853-006-7408-8

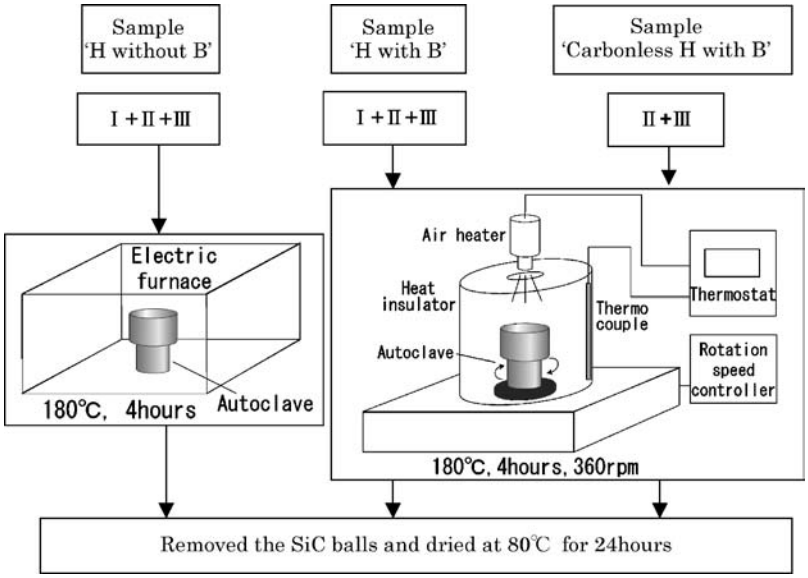

Figure 1 Experimental flowchart and design used in this study, I, II, and III indicate 0.50 g of activated carbon, 3 ml of 0.2 wt% of TAS-FINE and 100 SiC balls, respectively.

the ball milling and the addition of activated carbon on the morphology of the TiO_2 nano-particles.

2. Experimental methods

2.1. Sample preparations

A 2wt% solution of a titanium peroxocitric complex, TAS-FINE (Furuuchi Chemical Corp. Tokyo, Japan) was diluted with distilled water to a concentration of 0.2wt%. The precursor slurry for the hybrid material was prepared by mixing 3 ml of the TAS-FINE solution and 0.50 g of activated carbon (Takeda Chemical Industries, Ltd., Tokyo, Japan). The samples were prepared in one of three ways as shown in Fig. 1. In the first processing method, the slurry and 100 SiC balls of 5mm diameter were put into a 50 ml conventional autoclave which is composed of a Teflon (inner) and stainless steel (outer) vessel. The autoclave was then heated at 180°C, for 4 h while rotating at 360 r.p.m. using a planetary ball milling system (Centrifugal ball mill, Pulverisette6, FRITSCH Co., Ltd., Germany).

After finishing heating and rotating, the SiC balls were removed from the autoclave, then the samples were dried at 80 for 24 h in an electric oven. The sample after this process was called 'H with B'. In the second process, the slurry and 100 SiC balls were placed in an autoclave, same using the previous method, then the autoclave was heated in an electric furnace at 180°C, for 4 h without rotating. The other procedures were same as the first method. The sample from the second process was called 'H without B'. In the third process, the preparation of the sample was the same as that of 'H with B' except that the starting material was only 3ml of Ti solution (0.02wt%) without activated carbon. The sample from this process was called 'Carbonless H with B'.

2.2. Characterization methods

The characterization of the activated carbon and TiO_2 particles were performed by X-ray diffraction (XRD) using Cu K_α. (MXP3VA, MAC Science Co., Ltd., Tokyo, Japan), and micro Raman scattering at wavelength of 514.5 nm (T64000, Jonin Yvon Atago Bussan, Tokyo, Japan). The weight ratios of the activated carbon to TiO_2 particles were measured by Thermogravimetry and Differential Thermal Analysis (TG-DTA) (Type-2020, MAC Science Co., Ltd., Tokyo, Japan). The microstructure and crystallographic analyses were performed by Transmission Electron Microscopy (TEM) (JEM2000EX, JEOL Co., Ltd., Tokyo, Japan) using an acceleration voltage of 200 kV or High Resolution Transmission Electron Microscopy (HRTEM) (H-9000NAR, HITACHI Co., Ltd., Tokyo, Japan) using an acceleration voltage of 300 kV. Selected Area Electron Diffraction (SAED) of the TEM was performed in order to investigate the crystal growth direction of the TiO_2 particles. Gold polycrystals (FCC, $a = 0.4078$ nm) evaporated on a microgrid were used for collecting data for the electron diffraction pattern.

3. Results

3.1. XRD and Raman scattering

The XRD patterns of the three samples are shown in Fig. 2a. The samples prepared by 'H with B' and 'H without B' showed the (101) peak of anatase TiO_2 and

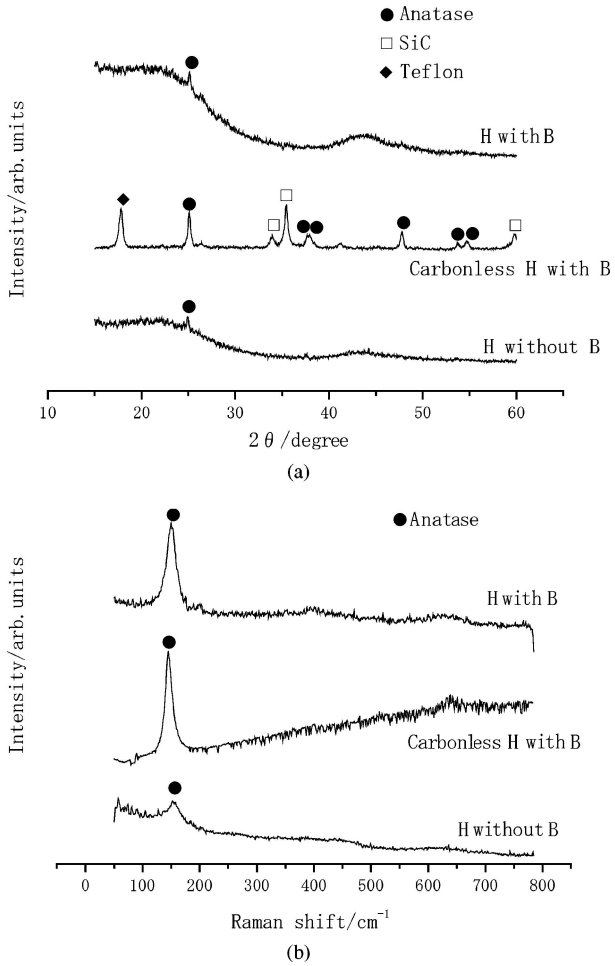

Figure 2 XRD patterns (a) and Raman scattering spectra (b) of the sample prepared by 'H with B', carbonless H with B' and 'H without B'.

broad peaks corresponding to amorphous activated carbon, whereas 'Carbonless H with B' showed the peaks of anatase, Teflon and alpha-SiC. The Raman scattering spectra for these samples are shown in Fig. 2b. All of the three samples showed signals of the characteristic scattering by anatase TiO_2.

3.2. TG-DTA

The TG-DTA analysis is shown in Fig. 3. There exists an endothermic peak with a weight decrease of about 1.50 mg in the temperature region of 30 to 90°C and a large exothermic peak with a large weight decrease of about 8.43 mg between 450 and 720°C. The weight of the remnant TiO_2 particles was 0.19 mg.

3.3. TEM and SAED

TEM images of the three samples are shown in Fig. 4. The samples prepared by 'H with B' and 'H without B' were composed of amorphous activated carbon and rectangular TiO_2 particles. The size of the TiO_2 particles in the sample

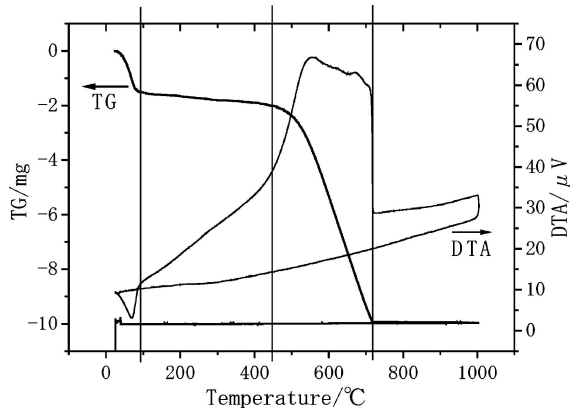

Figure 3 TG-DATA analysis of the sample prepared by 'H without B'.

prepared by 'H with B' was about 50 nm× 60 nm and 'H without B' was about 30 nm× 80 nm. The sample prepared by 'Carbonless H with B' was composed of alpha SiC particles (diffraction patterns are not shown) and rod-shaped TiO_2 particles with the size of about 40 nm × 300 nm. The corresponding SAED of each TEM image is shown in the box of each image in Fig. 4. The diffraction spots were detected as shown in each figure by the crystallographic analysis of each diffraction pattern. The HRTEM data of the sample of 'H without B' is shown in Fig. 5, in which the TiO_2 particle was rectangularly grown along the [001] direction. The size distributions for the longer and shorter axes of every TiO_2 particle are shown in Fig. 6, in which the longer axis is shown as the aspect ratio to the shorter axis length. The detection of the *a* axis and *c* axis for each TiO_2 particle in the TEM images was based on the assumption that the shorter axis is the *a* axis and the longer axis is the *c* axis. This assumption might include some errors, but the distribution from many particles can supply enough data to qualitatively discuss it. The average shorter-axis-length of the TiO_2 particles prepared by 'H with B', 'H without B' and 'Carbonless H with B' were 45 nm, 31 nm and 41 nm, respectively. The average aspect ratios of the TiO_2 particles prepared by 'H with B', 'H without B' and 'Carbonless H with B' are 1.2, 1.6 and 5.4, respectively.

4. Discussion

The XRD patterns and Raman scattering spectra in Fig. 2 show that the samples by 'H with B' and 'H without B' are composed of anatase TiO_2 and amorphous activated carbon, whereas that by 'Carbon-less H with B' is composed of anatase TiO_2, Teflon and alpha SiC. Alpha SiC and Teflon appear to be formed by the mechanical effects of the SiC balls with the Teflon wall due to breakdown during the ball milling. On the other hand, the other two samples contain activated carbon but neither alpha SiC nor Teflon.

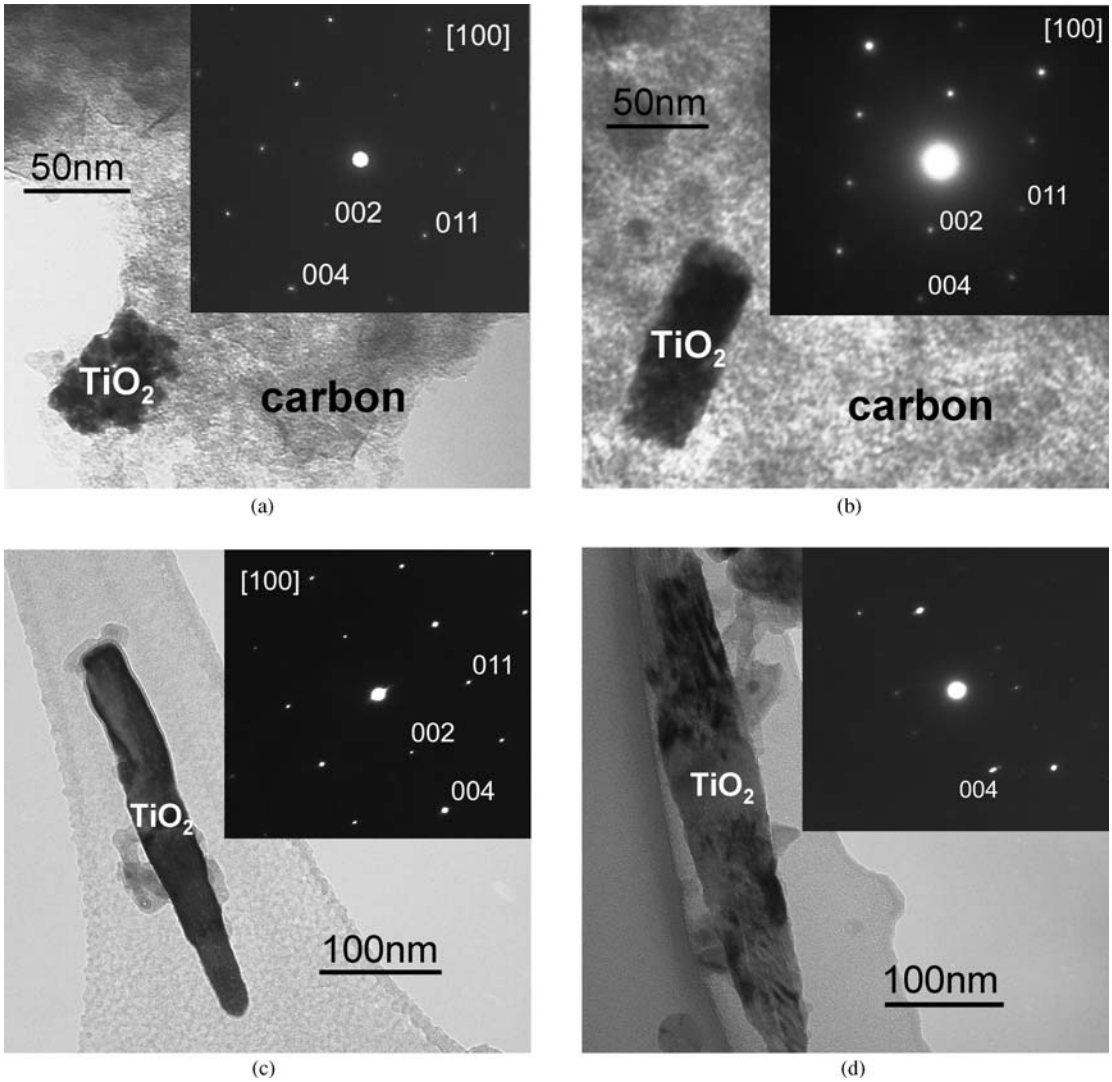

Figure 4 TEM images and corresponding SAED patterns of the sample prepared by (a) 'H with B', (b) 'H without B' and (c) 'Carbonless H with B'. (d) TEM images of TiO_2 particles prepared by 'Carbonless H with B' from an angle slightly different from [100], in which the SAED pattern of 002 disappeared.

These differences indicate that the activated carbon would work as a shock absorber for the SiC balls. Under the conventional milling conditions of dry powders, anatase TiO_2 can be transformed into the other form of TiO_2 by mechanochemical effects [11], thus, ball milling of the TiO_2 particles was considered to be a disadvantage for the photocatalytic activities. However, the milling and mechanochemical effects of the TiO_2 nano-particles would not be significant in the present experiments in which a large amount of aqueous solution and mechanically soft particles of activated carbon existed in the system. In fact, anatase particles formed in the present experiments were well crystallized nano-crystals as seen in the XRD, Raman scattering and TEM results. One can conclude that the role of the SiC balls was stirring rather than mechanochemical assistance for the TiO_2 nano-particles under the experimental conditions with a sample containing activated carbon. From the Raman scattering data, TiO_2 particles precipitated from solution seemed to nucleate on the surface of the amorphous carbon because Raman scattering is the only data from the surface of the substances.

In Fig. 3, the weight decrease vs. the endothermic peak in the temperature region of 30 to 90°C, indicates the evaporation of water, whereas the weight decrease vs. the exothermic peak between 450° and 720°C, indicates the oxidization of activated carbon. Its weight decrease between 450° and 720°C, of 8.43 mg well corresponded to the weight ratio of the starting materials, 98wt.% activated carbon and 2wt% TiO_2. Much higher TiO_2 contents are required for practical applications as photocatalysts.

Fig. 4 show that the shapes of the TiO_2 particle prepared by 'H with B' are more isotropic than those of 'H without B' and 'Carbonless H with B', because the SAED of each TiO_2 particle showed a zone axis of [100] in all three samples although the TEM images are two

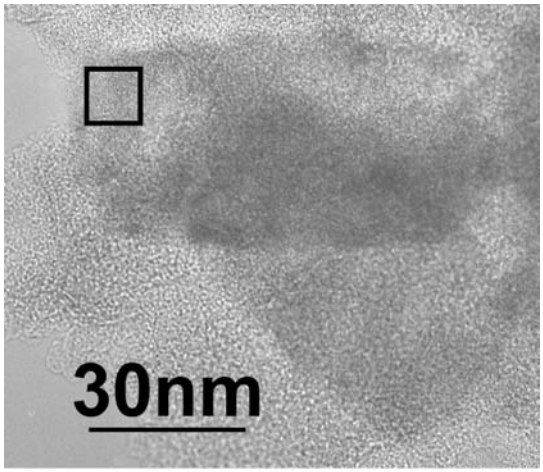

(a)

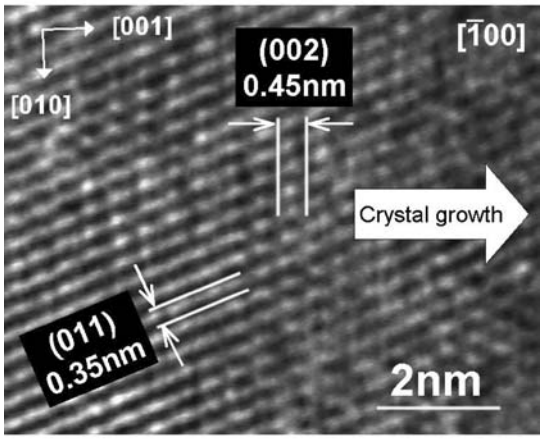

(b)

Figure 5 HRTEM images of the sample prepared by 'H without B' (a) and enlarged view in boxed area (b). Direction of crystal growth is parallel to the anatase [001].

dimensional images. There exists an angle differences about 13 degrees between the growth direction of the TiO_2 particles in the bright field image and the [001] direction of the corresponding SAED. However, we could consider these two directions to be the same because it was confirmed for the HRTEM image of the TiO_2 particle for the sample of 'H without B'. These differences might be caused by the rotating of the electron beam between the bright field image and SAED.

One can see the spots of the 002 planes in Fig. 4, which should disappear according to the extinction rule. This is, however, not uncommon because in practical situations they do appear due to dynamic diffraction or double diffractions as reported by Chang *et al.* [12]. The SAED of the TiO_2 crystal in Fig. 4 (d), which turned around the [001] axis, confirmed that the 002 spots appeared by the dynamic diffraction or double diffractions. If these spots were caused by the kinematic diffraction, they should remain without dissipating by rotation along the c axis. Fig. 5 indicates that the TiO_2 particles prepared by 'H without B' have a tendency to grow along the [001] direction and those by the 'Carbonless H with B' have a great tendency of growth compared to that of 'H with B'. The difference in the TiO_2 particle sizes between the two samples of 'H with B' and 'Carbon-less H with B' seems to be caused by the difference in the possible nucleation in the solution. Activated carbon particles would prepare heterogeneous nucleation sites for TiO_2, thus the 'H with B' condition would produce more nuclei then the smaller particles of 'carbonless H with B'. The difference in the TiO_2 particle sizes between the samples 'H with B' and 'H without B' might be caused by stirring. In both cases, the nucleation of TiO_2 should occur at a similar supersaturation but the crystal growth rate should be accelerated due to stirring in 'H with B', in which the TiO_2 crystals have grown larger but less heterogeneous along the [001] direction due to

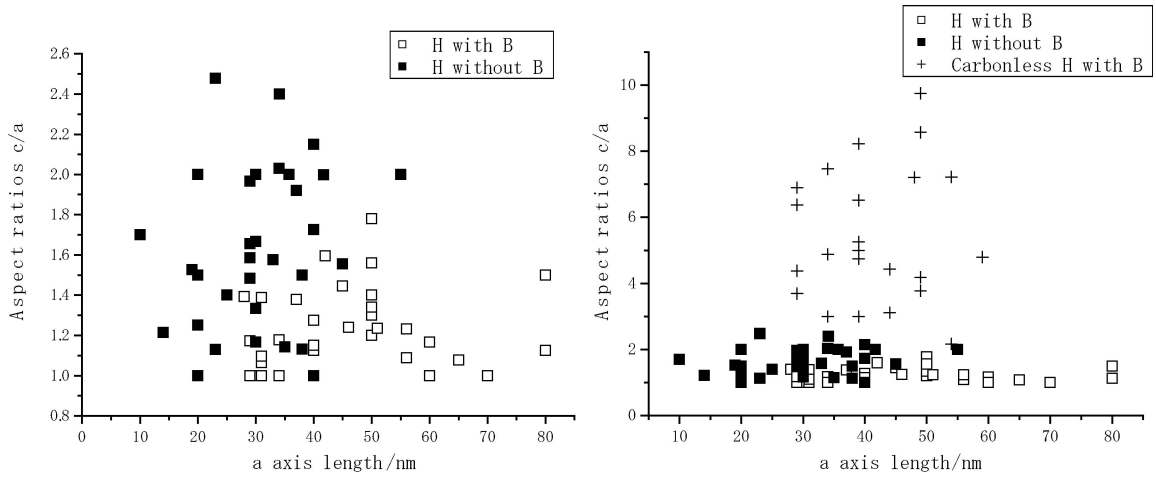

Figure 6 Distribution of the TiO_2 particle sizes along the *a* axis and aspect ratio c/a for the samples prepared by (a) 'H with B' and 'H without B' and(b) Carbonless ('H with B' and 'H without B' also shown).

faster growth by stirring than for the case without stirring in 'H without B'. As described above, we can control the morphology and size of the TiO_2 particles by controlling the experimental conditions. The present method might have another advantage over the other conventional methods [2–5] from environmental and economic points of view, because it can produce shape and size controlled TiO_2 particles in a single step under hydrothermal conditions.

5. Conclusion

Hybrid materials of anatase and activated carbon could be prepared by the 'H with B' method in a single step at 180°C. It was concluded that

1. TiO_2 particles heterogeneously nucleated by the activated carbon.

2. TiO_2 particles have a tendency to grow along the *c* axis under the stated experimental condition.

3. The crystal growth direction of the TiO_2 particles can be isotropically controlled less heterogeneously by the ball milling.

The present 'H with B' method can be performed in a conventional autoclave with SiC balls, thus it has advantages from environmental and economic points of view compared to other methods for fabricating hybrid materials of TiO_2 and activated carbon.

Acknowledgments

The authors acknowledge Dr. Y.Shinoda and Ms. T. Aoyama of the Tokyo Institute of Technology for their advice during the TEM and HRTEM analyses. They are also thankful to Dr. A.Ahniyaz of the Tokyo Institute of Technology for the experimental ball milling setup.

References

1. M. ANPO, *Catal. Surv. from Japan* **1** (1997) 169.
2. H. YONEYAMA and T. TORIMOTO, *Catal. Today* **58** (2000) 133.
3. Z. DING, X. HU, P. L. YUE, G. Q. LU and P.F. GREENFIELD, *ibid.* **68** (2001) 173.
4. H. YAMASHITA, M. HARADA, A. TANII, M. HONDA, M. TAKEUCHI, Y. ICHIHASHI, M. ANPO, N. IWAMOTO, N. ITOH and T. HIRAO, *ibid.* **63** (2000) 63.
5. K. BYRAPPA, A. K. SUBRAMANI, K. M. L. RAI, B. BASAVALINGU, S. ANANDA and S. SRIKANTASWAMY in Procceedings of International School on Crystal Growth of Technologically Important Electronic Materials, (Mysore, India, 2003) p. 291.
6. T. WATANABE, W. S. CHO, W. L. SUCHANEK, M. ENDO, Y. IKUMA and M. YOSHIMURA, *Solid State Sci.* **3** (2001) 183.
7. T. FUJIWARA, Y. NAKAGAWA, T. NAKAUE, S. W. SONG, T. WATANABE, R. TERANISHI and M. YOSHIMURA, *Chemi. Phys. Lett.* **365** (2002) 369.
8. M. YOSHIMURA, W. L. SUCHANEK and K. BYRAPPA, *MRS Bulletin*, **25**(9) (2000) 17.
9. J. PREZEPIORSKI, N. YOSHIZAWA and Y. YAMADA, *J. Mater. Sci.* **36** (2001) 4249.
10. P. SUJARIDWORAKUN, D. PONGKAO, A. AHNIYAZ, Y. YAMAKAWA, T. WATANABE and M. YOSHIMURA, *J. Nanosci.* in press (2005).
11. S. B. COLIN, T. GIROT, A. MOCELLIN and G. L. GAER, *NanoStruct. Mater.* **12** (1999) 195.
12. H. L. M. CHANG, T. J. ZHANG, H. ZHANG, J. GUO, H. K. KIM and D. J. LAM, *J. Mater. Res.* **8** (10) (1993) 2634.

Received 04 February
and accepted 19 April 2005